N69-33589
CR-103854

SEMIANNUAL REPORT

FOR

SOLAR CELL RESEARCH

15 October 1968 - 16 April 1969

CONTRACT NO. WO-8056

NAS 7-100

PREPARED BY

NAVAL RESEARCH LABORATORY
SOLID STATE APPLICATIONS BRANCH
WASHINGTON, D.C. 20390

SEMIANNUAL REPORT

FOR

SOLAR CELL RESEARCH

15 October 1968 - 16 April 1969

CONTRACT NO. WO-8056

NAS 7-100

PREPARED BY

NAVAL RESEARCH LABORATORY
SOLID STATE APPLICATIONS BRANCH
WASHINGTON, D.C. 20390

This work was performed for the Jet Propulsion Laboratory, California Institute of Technology, as sponsored by the National Aeronautics and Space Administration under Contract NAS 7-100.

This report contains information prepared by the Naval Research Laboratory under JPL subcontract. Its content is not necessarily endorsed by the Jet Propulsion Laboratory, California Institute of Technology, or the National Aeronautics and Space Administration.

Approved by: 

E. L. Brancato
Project Supervisor

ABSTRACT

This report covers the first six months of progress on solar cell research.

(1) Thermal annealing at room temperature of radiation damage induced in lithium-diffused silicon by 1 MeV electrons at 77°K was studied by Hall effect measurements. The results indicated that both lithium (Li^+) and lithium paired with oxygen (LiO^+) are available for the annealing of damage.

(2) A study of low flux Co^{60} gamma irradiation of lithium-diffused silicon solar cells has revealed the presence of a continuing damage stage in the cell parameters after prolonged exposure.

(3) Successful implantation of boron in a silicon semiconductor device has been achieved by means of a focused controlled boron ion beam.

(4) Preliminary measurements of the parametersof silicon solar cells at 80°K have indicated that the cell efficiency generally improves with decreasing temperature; however, in some instances, cell contacts have exhibited non-ohmic behavior below 200°K.

(5) A computer program has been written for analyzing the diode parametersof a solar cell by a least-squares fitting process of I-V data to the solar cell equation.

(6) Chapters II and II of the Handbook on Space Environmental Effects on Solar Cell Power Systems have been reviewed.

TABLE OF CONTENTS

SECTION	TITLE	PAGE
1.0	INTRODUCTION	1
2.0	DISCUSSION	3
2.1	Radiation Effects in Lithium Diffused Silicon	3
2.2	Low Flux Gamma Radiation of Lithium Diffused Solar Cells	16
2.3	Solar Cell Contacts	20
2.4	Electrical Characteristics of Silicon Solar Cells at Low Temperature	24
2.5	Analysis of Solar Cell I-V Characteristics	26
2.6	Review of "Handbook of Space Environmental Effects on Solar Cell Power Systems"	30
3.0	CONCLUSIONS	33
4.0	RECOMMENDATIONS	35
5.0	NEW TECHNOLOGY	37
6.0	PUBLICATIONS (Written and Oral)	38
7.0	REFERENCES	39

ILLUSTRATIONS

FIGURE	TITLE	PAGE
1	Two Impurity Model	5
2	Carrier Concentration After Irradiation And Annealing	7
3	Defect Concentration Vs. Annealing Time	8
4	Effect of Annealing on Fermi Energy	9
5	Effect of Annealing on Defect Concentrations	11
6	Relative Changes in Acceptor and Donor Concentrations	13
7	Deep Donor Annealing	14
8	Deep Donor Energy and Carrier Concentration	15
9	35 KeV Ion Accelerator	21
10	Mass Scan of BCL_3	23
11	Low Temperature Mount for Solar Cells	25
12	Computer Fit of I-V Curve	29

TABLES

TABLE	TITLE	PAGE
I	Experiment Sample Matrix	18
II	Proposed Experiment Sample Matrix	36

I. 0 INTRODUCTION

The major portion of the research program comprises a number of study areas which are directed toward understanding and improving the radiation resistance of silicon solar cells. These areas of study include investigating radiation effects in silicon crystals (e.g. the behavior of lithium in silicon), studying problems relating to the surface properties of silicon (e.g. contact techniques), and the measurement and evaluation of properties of manufactured solar cells.

The objective of the bulk silicon study is to develop a better understanding of the radiation damage model for lithium-diffused solar cells. The approach to this task is to utilize the measurement of Hall coefficient in irradiated lithium diffused silicon as a function of temperature, fluence, and post-irradiation thermal annealing time. During the first six months reporting period, this has proven successful in identifying the energy level and annealing kinetics of donor and acceptor states in float-zone silicon doped with lithium.

Another aspect of the effect of lithium in irradiated silicon is under investigation. In this experiment, the properties of lithium-diffused silicon solar cells are evaluated as a function of temperature and radiation at low flux rates. For the period of this report, this particular work was a continuation of an experiment initiated in June 1967 at GSFC. This experiment was terminated and the experience gained has led to a better designed experiment which is being assembled.

During the recent past, solar cell contact problems have been recognized as a serious source of space power system failure. One phase of the present contract relevant to this situation is the development of improved silicon solar cell contacts, employing ion implantation and sputtering techniques. In the first six months, a 30 KeV boron beam has been developed and successfully utilized to implant boron atoms in a semiconductor device. Some progress has been made in obtaining a metallic ion source.

With respect to evaluating solar cell properties (in addition to the Co^{60} radiation experiment), NASA has requested that we study silicon solar cell parameters as a function of temperature and illumination at conditions corresponding to a Jovian environment. This requires cell temperatures at least as low as 125°K and illumination intensities of $5 mW/cm^2$. This request was made after the initiation of the contract. Apparatus has been made ready for this work and some measurements have been done.

Another phase of the study of solar cell characteristics is being carried out by means of detailed analysis of the I-V curve using computer techniques. Through a curve-fitting procedure using the diode equation, and photovoltaic current-voltage data, the best-fit values for R_S, I_O, A, and I_L can be obtained. The computer program has been written and some analysis has been performed.

Finally, one task in the contract is to review the Handbook of Space Environmental Effects on Solar Cell Power Systems for applicability by power systems engineers. In the present report, Chapters II and III, entitled "The Theory of the Silicon Solar Cell" and "Instrumentation Techniques for Measuring Solar Cell Parameters", respectively, are reviewed.

2.0 DISCUSSION

2.1 Radiation Effects in Lithium-Diffused Silicon

The Hall effect has been used extensively to measure impurity and damage center concentrations in semiconductors. In fact it is still the most sensitive tool available for such determinations. When performed as a function of temperature between 4°K and 300°K on a semiconductor containing one type of acceptor and one type of donor, the measurement allows a separate determination of these two concentrations. In addition the location of one of the levels in the forbidden gap may be determined. Hall effect studies of radiation damage in lithium doped silicon until now have been limited to temperatures above 77°K. Such a measurement allows a quantity equal to the donor concentration minus the acceptor concentration to be determined. This means the creation of an acceptor affects the measured quantity in the same way as the loss of a donor. Both of these processes are presumed to occur for radiation damage in Si(Li) and cannot be separated in a measurement restricted to high temperatures. The experiment to be described here was designed to separate these effects by making Hall effect measurements over the full range 4°K to 300°K.

Preliminary work had indicated that 1-MeV electron irradiation of F. Z. silicon containing 10^{16} lithium/cc, and performed at 300°K, did not cause the increase in acceptor concentration expected from present models of radiation damage. A similar experiment but with the irradiation performed at 80°K did show an increase in acceptor concentration. These results indicated that to separate the effects of damage from those of annealing, irradiation must be performed at low temperature. In this experiment the sensitivity of the Hall effect was exploited by using a sample which contained less than 10^{14} lithium/cc. This provided two major advantages. First the anomalous dependence of the Hall constant on temperature characteristic of heavily irradiated material was avoided. Secondly it was arranged so that at some point in the experiment the free lithium would be depleted. This last point proved to be vital to the success of this experiment.

Before discussing experimental results, some comments on the Hall effect at low temperatures and in particular the application of this tool to damaged material is in order. Hall effect allows the carrier concentration to be measured to within a proportionality factor known as the Hall factor. This is a function of temperature and magnetic field varying between .9 and 2 in magnitude. Under the conditions of this experiment the Hall effect may be assumed to give the carrier concentration directly for temperatures below 100°K. Above 100°K corrections were necessary. The statistics relating

carrier concentration to defects present in the solid require two adjustable parameters, concentration and ionization energy, for each type of defect. In the case of material damaged by radiation a wide variety of defects are present, causing an exact theory to involve large numbers of adjustable parameters. In this experiment a simple four parameter model presuming only one type of acceptor and one type of donor was used to fit the data. The applicability of this model can best be seen intuitively by considering the situation which exists at absolute zero. This condition of minimum energy which is shown in Figure 1 is reasonably accurate to 40°K in Si (Li). Several types of donors and acceptors are shown in the forbidden gap of silicon. An electron added to this system would fill the lowest lying unfilled state. The choice of which level will be partially occupied is determined entirely by the balance between the number of acceptors of lower energy and donors of higher energy. If acceptor states deep in the gap are added in sufficient quantity the partially filled defect may become entirely depopulated causing a deeper lying level to become partially filled. However the addition of a donor deep in the gap affects nothing and is not detectable. The Fermi level is that position in the gap where the probability for a level to be filled is 1/2. In general this is fixed very near that level which is partially occupied. As a result a measurement of the depth of the Fermi level below the bottom of the conduction band can give the ionization energy of the partially filled level. As temperature is increased from 0°K the population of only those levels within kT of the Fermi energy change. The use of a two impurity model with four parameters, N_A, N_D, ionization energy and degeneracy factor is rationalized as follows. The acceptors in the lower half of the gap are always filled so their presence can be approximated by a single acceptor level of concentration N_A. The donors near the conduction band are assumed to be one type of donor lying at the energy of the partially filled donor and with a concentration equal to the sum of the separate densities. The fact there are really not N_D donors at this energy but a smaller number, causes a physically unrealistic value of the degeneracy factor to be obtained when the two impurity model is fit to the data. Degeneracy factors of as low as 1/60 where obtained where 1/2 is expected theoretically. The validity of this model was verified by fitting it to false data calculated assuming three impurities. These results indicated concentrations were accurate to within 20 to 30%. However, this model is less accurate when the Fermi level is part way between two levels of similar ionization energy, both of which are partly occupied.

The plan of this experiment is as follows. A sample of 100-Ωcm F. Z. silicon was doped with lithium by diffusion to a total donor concentration of 10^{14}/cc. The ratio of the concentration of lithium to that of phosphorus was

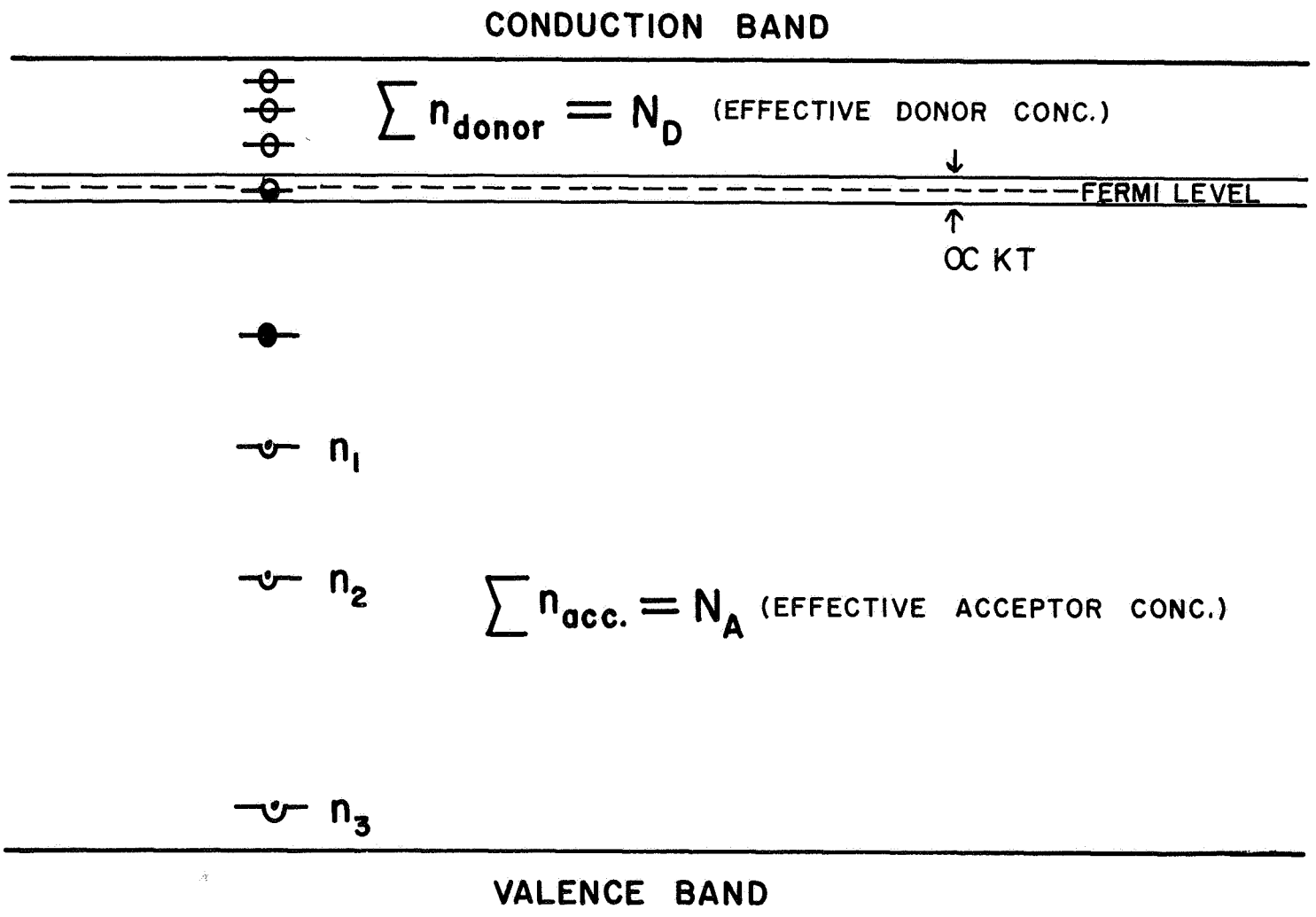

Figure 1. The forbidden gap of silicon is shown with various impurity and defect states present in the gap. Electronic occupations shown are characteristic of very low temperature as is the indicated position of the Fermi level. In the two impurity models the acceptor and donor concentrations are summed to give the two parameters N_D and N_A.

about two to one. After Hall measurements were made it was irradiated at 77°K with 4 x 10^{14} 1-MeV electrons/cm^2 and remeasured. Subsequently it was remeasured after annealing at 200°K to remove intrinsic defects and after five periods of increasing duration at 300°K. The resultant data were fit to a two impurity model with four adjustable parameters using the method of least squares. It was not possible to include a control sample of Si(P) to guard against anomalous annealing not due to lithium. The effects of this on the conclusion will be noted as they arise.

The results obtained from measurements made below 100°K are discussed first. Experimentally determined electron concentration as a function of inverse temperature is shown in Figure 2. Electron concentration changed over eight orders of magnitude as the temperature changed from 100°K to 14°K. The low temperature limit was set by the inability of the apparatus to measure potentials from a source whose impedance was greater than 10^{10} ohms. The slope of the curves in the linear portion represents the Fermi level at low temperature. Comparison of these curves shows the Fermi energy moved deeper into the gap as the experiment proceeded. The value of the electron concentration at high temperature equals (N_D-N_A) and decreased on annealing at 300°K. The form of this decrease was in agreement with the carrier removal studies by Carter.[1]

The explicit dependence of the donor and acceptor concentrations on time of annealing at 300°K is shown in Figure 3. Donor and acceptor concentrations are represented by the upper and lower traces respectively. Both show a decrease with annealing time. The acceptor concentration decreases a full order of magnitude, until after 1500 hours it is near the acceptor concentration measured before irradiation. The majority of the acceptor concentration indicated here is due to the irradiation and it does anneal at room temperature. Two points shown off scale to the left represent the values measured after annealing at 200°K. Large error in the point corresponding to 61 hours is attributed to the fact the Fermi level at low temperature was located midway between the energy levels of the free [Li] donor and the [Li 0] pair donor. The decrease in acceptor concentration shown is vital to the argument presented with Figure 4.

During the course of the experiment the Fermi energy at low temperature moved deeper into the gap. At the same time the donor concentration decreased. The points shown were obtained in sequence moving from right to left. As annealing proceeded the Fermi level moved from the vicinity of the lithium donor level to that of the lithium-oxygen donor. Then as the donor concentration approached the initial phosphorus concentration the Fermi

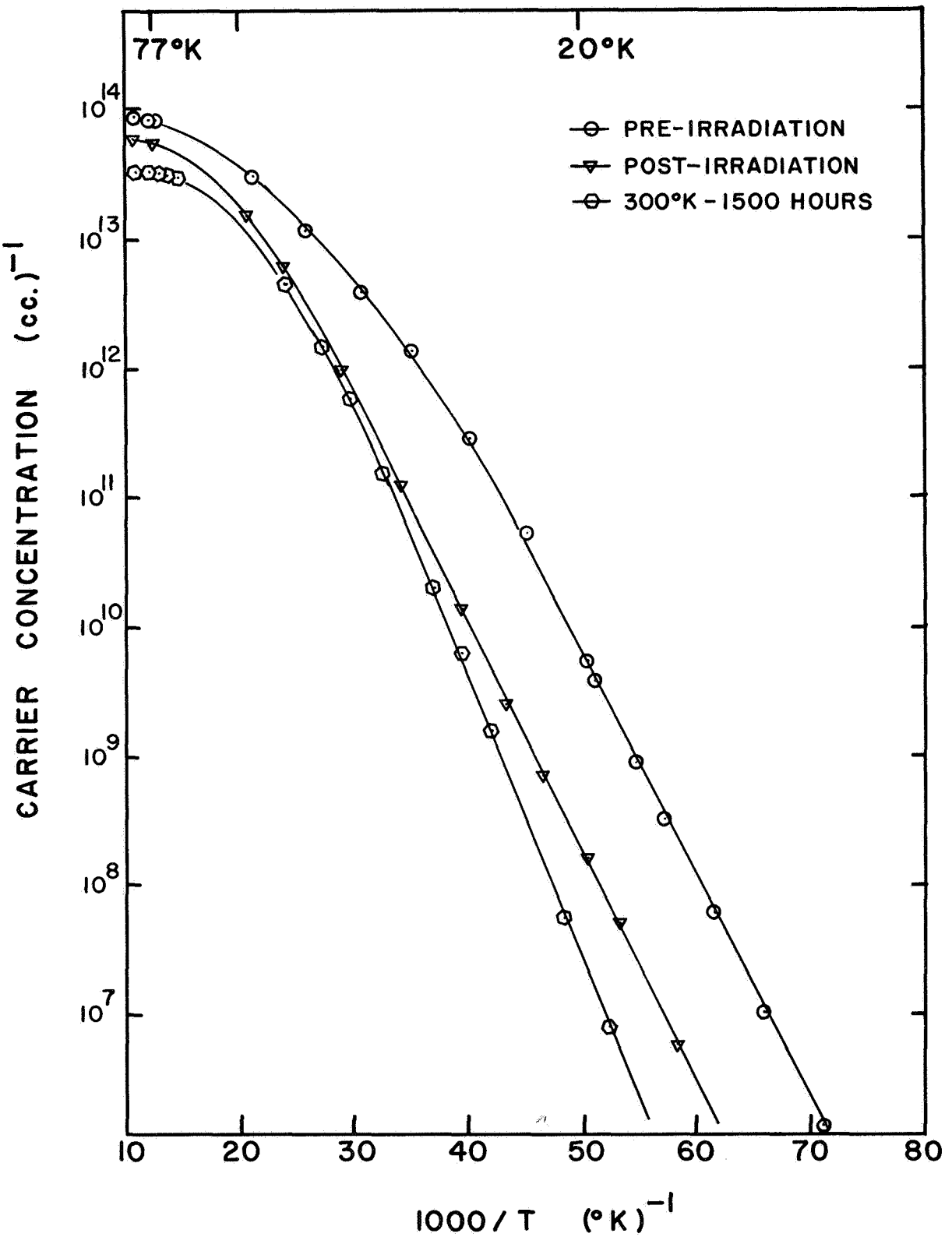

Figure 2. The effect of irradiation and annealing on the temperature dependence of carrier concentration is shown. Indicated curves were obtained by fitting the data to a two impurity model in the four adjustable parameters.

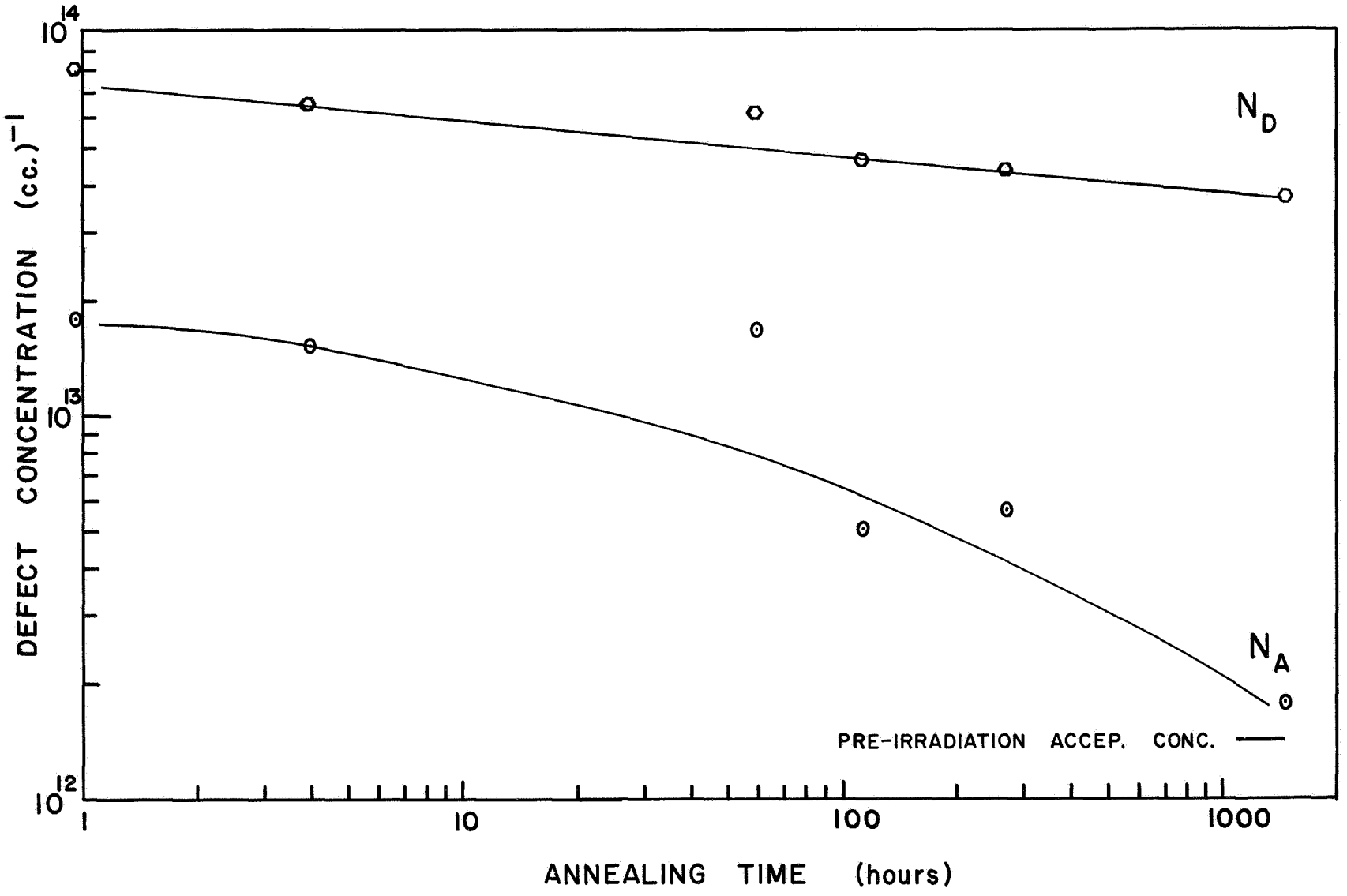

Figure 3. Annealing at 300°K caused both the acceptor concentration, N_A, and the donor concentration, N_D to decrease. After 1500 hours the acceptor concentration had returned almost to its pre-irradiation value.

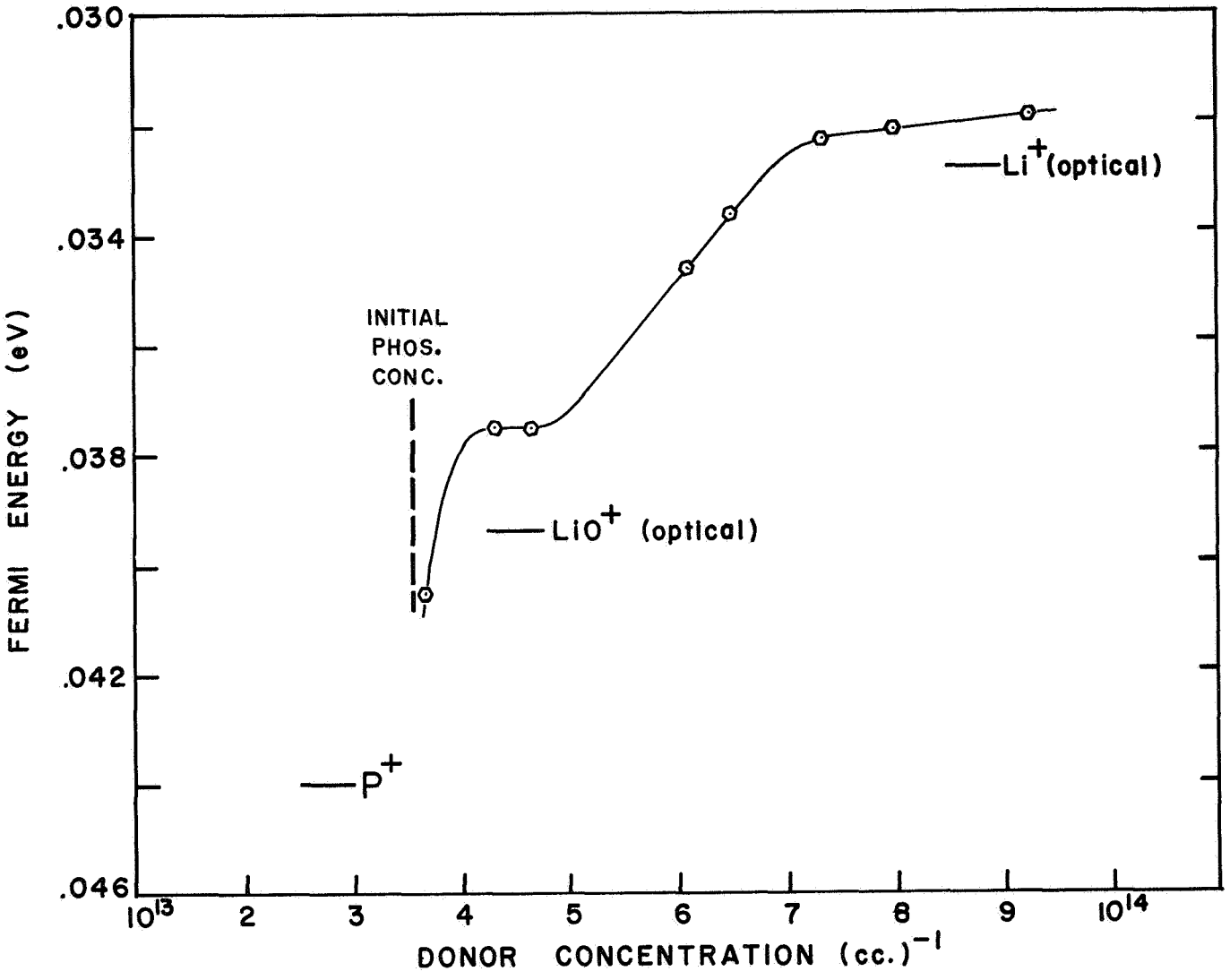

Figure 4. The movement of the low temperature Fermi energy as measured from the bottom of the conduction band is shown with change in donor concentration. Data was obtained in a sequence starting at the upper right. Pinning of the Fermi level near the optical excitations energies of Li^+ and LiO^+ identifies the donor level. Movement of the Fermi level through these levels indicates the concentration of each donor decreases strongly.

energy began to move toward the phosphorus donor level. This movement of the low temperature Fermi energy through a donor level can be brought about by either a large decrease in the concentration of that donor or an increase in acceptor concentration, thereby depopulating that donor completely. Figure 3 shows that the acceptor concentration was in fact decreasing not increasing, thereby ruling out the second alternative. In addition the decrease in donor concentration presumed by the first alternative was observed. This data establishes that the free lithium concentration is depleted and subsequent to this the LiO concentration is similarly depleted. It would seem that free lithium is removed by some process and this drives the lithium-oxygen pairing reaction to completion in the direction of decreasing lithium-oxygen pair concentration. Several more interesting points can be made here. First, if it is assumed that the data shown here indicates the thermal ionization energies of the [Li] and [LiO] donors, the differences between thermal and optical values is found to be about 1 meV for [Li] and 2 meV for [LiO] as compared to the known difference of 1 meV for phosphorus. This seems quite reasonable within the frame work of the Franck-Condon principle which is used to explain this difference between thermal and optical values. Secondly the times required for the depletion of the LiO donor are an order of magnitude greater than that required to deplete the free Li. Free Li is depleted in 100 hours or less while LiO donors are almost gone by 1500 hours.

Thirdly, when the Fermi level is near the LiO donor it can be stated that the free Li concentration must be less than the measured acceptor concentration. Using Pell's dissociation constant an estimate is obtained that the oxygen concentration must be greater than about 2×10^{15}/cc. Infrared absorption measurements were performed and showed no 9μ absorption other than that attributable to the lattice. This is as would be expected for F. Z. material. Finally while this is float zone material in oxygen content the behavior of the lithium is somewhat characteristic of pulled silicon. That is the free lithium content is at least partly determined by the dissociation of lithium oxygen pairs.

However, it must not be presumed that the lithium is lost due to precipitation as was the case in Pell's work with unirradiated pulled material. There the lithium concentration was orders of magnitude greater than the solid solubility for free lithium and the donor concentrations remained always above this solid solubility. Data in Figure 3 is shown again in Figure 5 in order to demonstrate that something quite different is occuring in this sample. Since the total donor concentration is less than four times the solid solubility of Li at 300°K, precipitation can be neglected. In addition the donor concentration falls below the solid solubility for lithium. Clearly some extremely active center is removing free lithium.

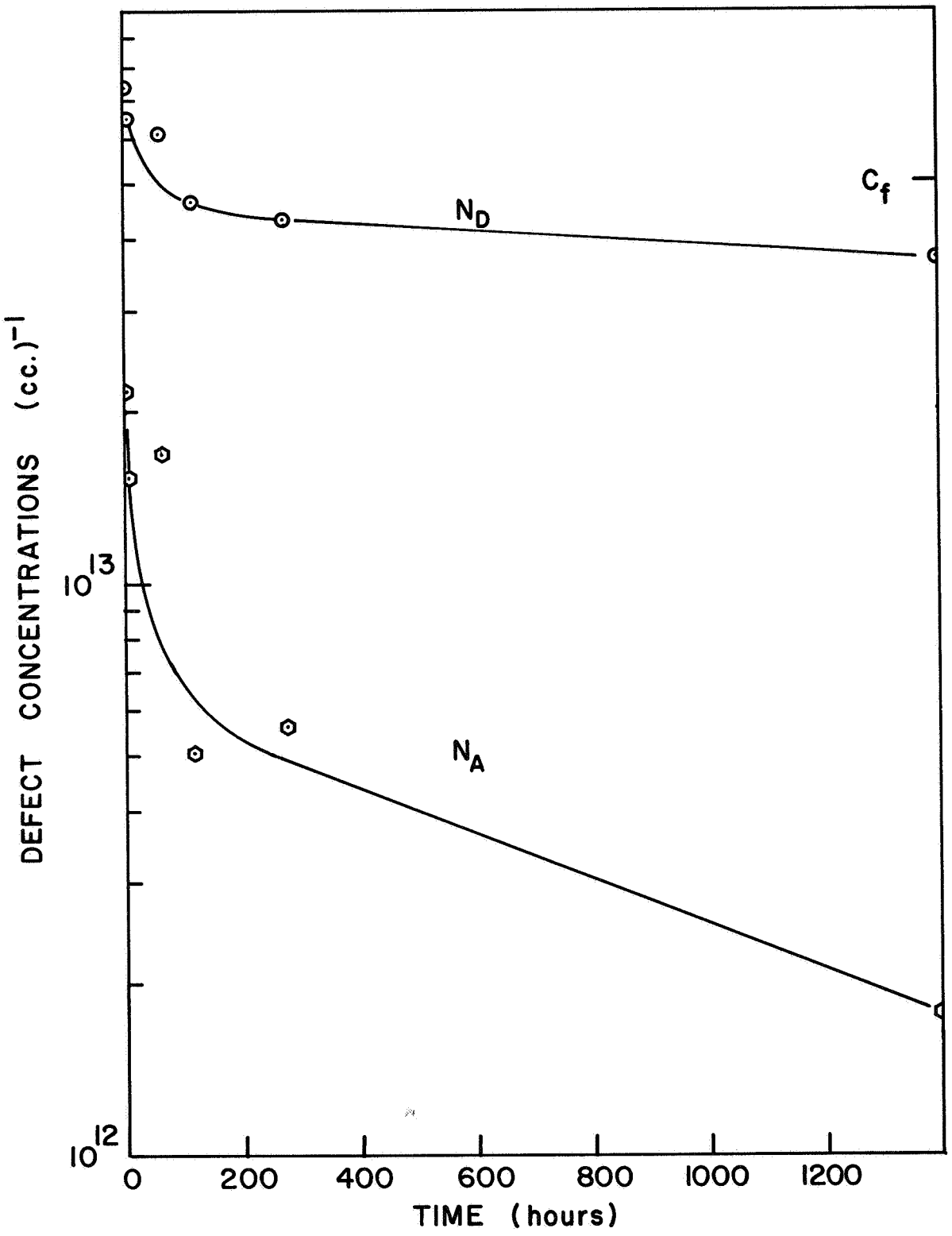

Figure 5. Data of Figure 3 is replotted to show precipitation is not causing the decrease in N_D. If precipitation were important N_D would not fall below the value indicated by C_F.

One further point can be made concerning the sinks to which the lithium is being removed. What is the relationship between the lithium loss and acceptor loss? The answer is that in both the slow and the fast parts of the annealing process approximately two donors were lost for each acceptor neutralized. If the change in acceptor concentration between time zero and time T is added to the donor concentration at time T the lower curve of Figure 6 is obtained. If twice the integrated acceptor change is added to the donor concentration the upper, nearly flat curve is obtained.

As the temperature is increased above $40^{\circ}K$ the Fermi energy tends to move downward toward the center of the gap. At $300^{\circ}K$ it can be as low as .3 eV below the bottom of the conduction band. At such high temperatures the concept of filled versus unfilled loses meaning. Suffice it to say that if the Fermi level passes through a level as it moves downward the population of that level will change and will thus produce a structure in the Hall data. Corrections for the Hall factor were necessary and were made using the Hall factor determined from the data taken before irradiation.

Structure due to A centers at .185 eV below the conduction band was not observed in measurements made after 61 hours at $300^{\circ}K$. Structure due to a deep level was observed however and its effect on the Hall data is shown in Figure 7. The various curves were taken at the indicated annealing times. Analysis indicates a concentration of about 1.5×10^{13}/cc and is apparently independent of annealing time. This level may well have been present immediately after irradiation. Also since its concentration far exceeds the acceptor concentration measured from the low temperature data it must be concluded that this center is a donor. As such it was neutral and undetected for all the measurements made below $100^{\circ}K$. The depth of this level can be seen from Figure 8. The dotted lines are carrier concentrations calculated for several values of deep donor ionization energy. Apparently the shape of the data agrees well with theory and the level is near .15 eV below the conduction band. Structure due to the A center would be near the .19 eV curve and is clearly not observed. Since there was no control sample the importance of Li to this donor is an open question.

The following conclusions can be made:

(1) Acceptor defects introduced in silicon containing lithium and phosphorus do become electrically neutral on annealing at $300^{\circ}K$.

(2) A decrease in concentration of both free lithium and lithium-oxygen pairs occurs concurrently with the decrease in acceptor concentrations.

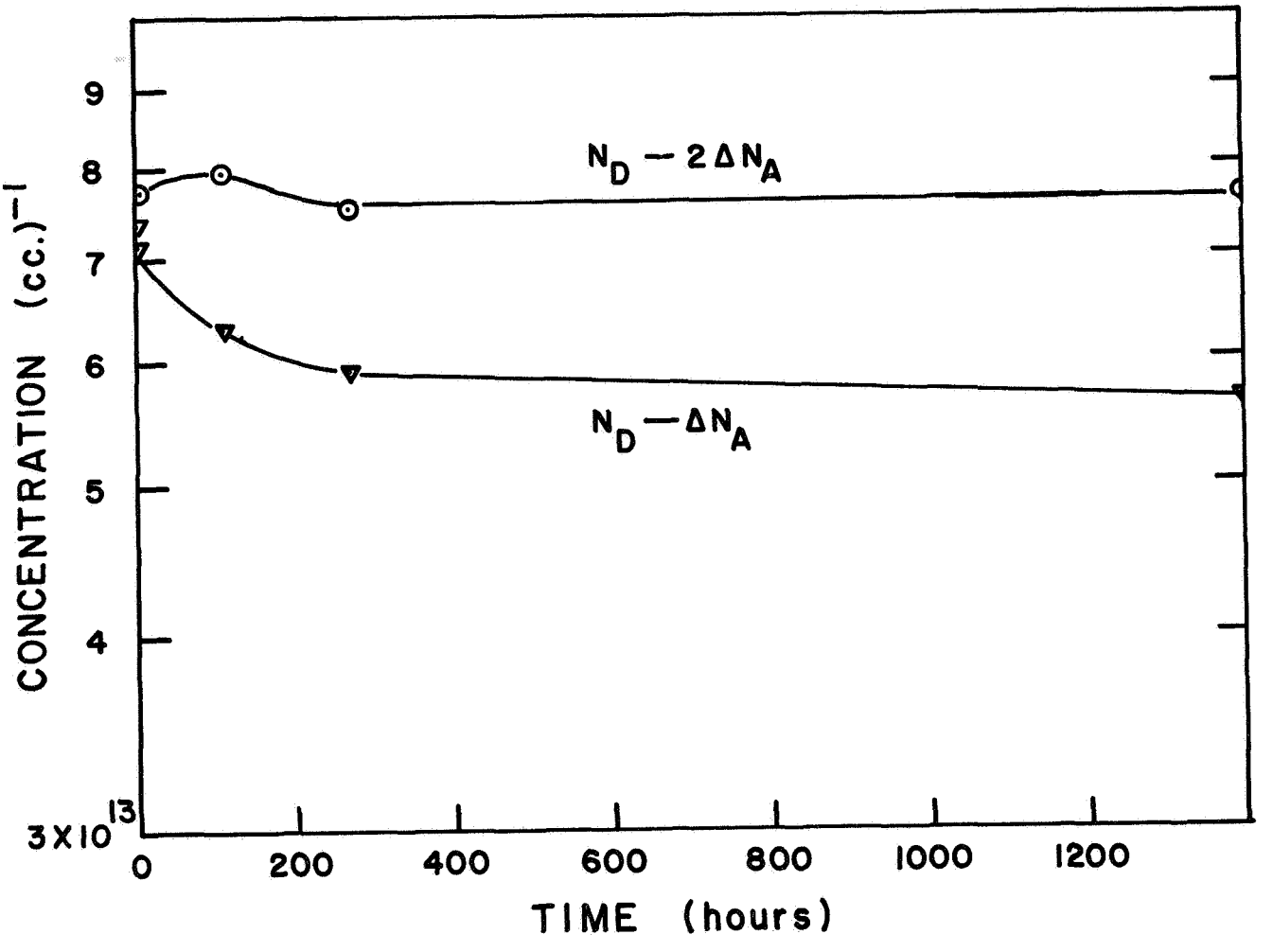

Figure 6. The relationship between the changes in N_A and N_D is shown. When the total decrease in N_A observed at each annealing time is added to the donor concentration at that annealing time the lower curve is obtained. Since this curve decreases it is clear that $\Delta N_D > \Delta N_A$. When $2\Delta N_A$ is added to N_D however the upper, approximately flat curve is obtained.

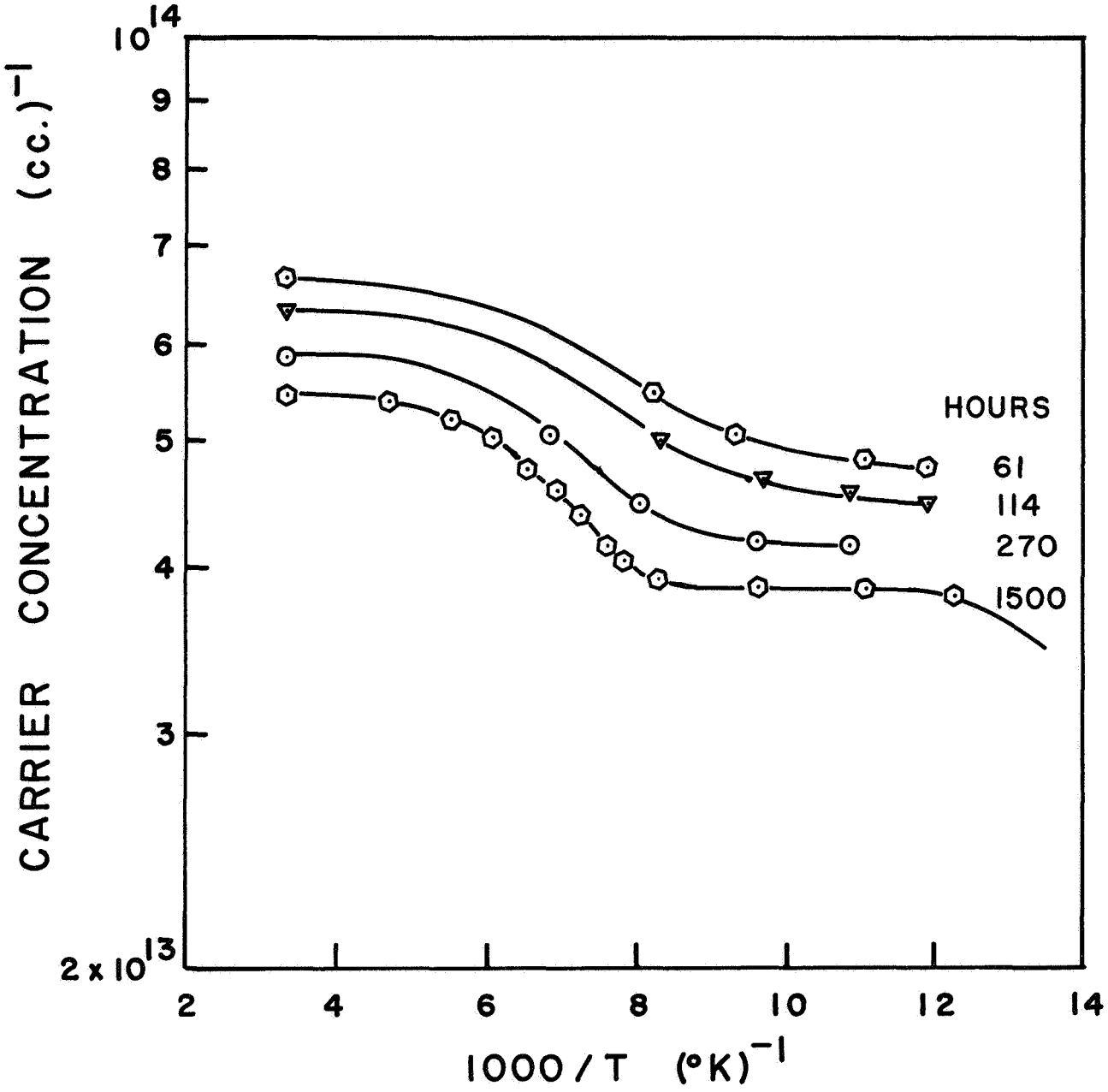

Figure 7. Data similar to that of Figure 2 but for temperatures above 80°K is shown. The several curves indicate a deep donor level whose concentration is relatively independent of annealing at 300°K.

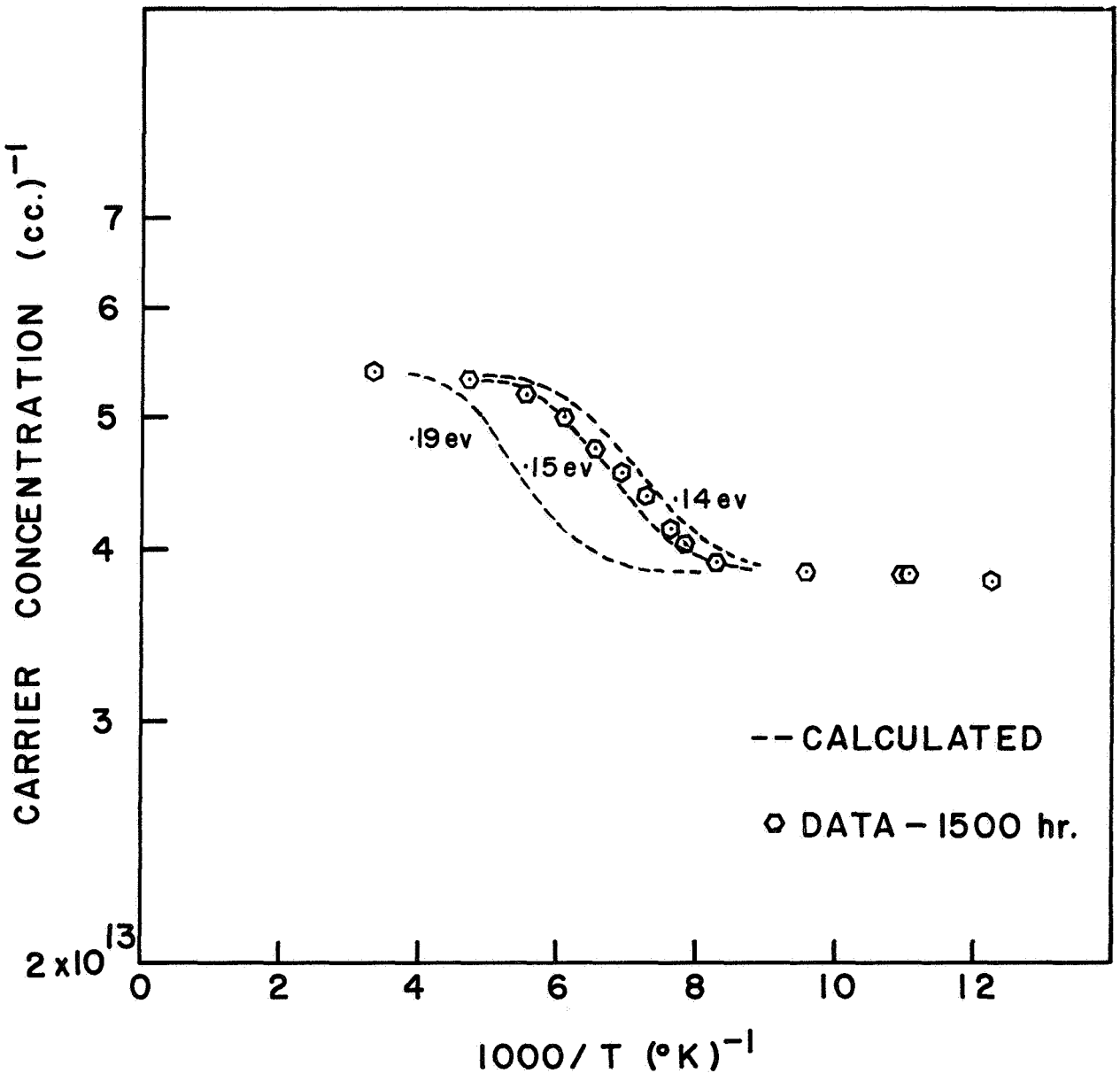

Figure 8. Data for 1500 hours taken from Figure 7 is shown along with calculated curves assuming three values of deep donor ionization energy. The deep donor has an ionization energy near .15 eV.

(3) Lithium is removed much more strongly than would be expected from a mechanism such as precipitation.

(4) In all phases of the annealing process the loss in donor concentrations was approximately twice the loss in acceptor concentrations.

(5) A deep donor level .15 eV below the conduction band was observed. Its concentration was independent of annealing at 300°K.

(6) No A centers were detected after 61 hours at 300°K.

2.2 Low Flux Gamma Radiation of Lithium-Diffused Solar Cells

This experiment was begun in June 1967 under the direction of P. Fang, Goddard Space Flight Center, NASA. The experimental work at that time was done by Electro-Mechanical Research, Ind. under NASA-GSFC Task 713-2220. It was continued until August 1968, at which time the EMR work was completed, following the departure of P. Fang from GSFC. NASA requested NRL to continue this experiment as long as it was useful.

The experiment consisted of Co^{60} gamma irradiation of a number of lithium and conventional solar cells in two evacuated chambers in a swimming pool source. Measurement of the total I-V curves under tungsten illumination of 100 mW/cm^2 solar equivalent were done on each cell at monthly intervals. The original plan in 1967 was to use solar simulation, but this had never been done. The final report of the EMR work was made on August 31, 1968.[2] The results of this were reported by Fang.[3] This present study is a follow-on from October 1968.

The cells had been irradiated by EMR at the National Bureau of Standards Co^{60} gamma pool. Because of pool water temperature change, the cells also varied over a temperature range in one chamber from 30 to 40°C and in the other chamber from 55 to 75°C. The test chambers were adapted to fit in the NRL pool, and placed on a vacuum system which maintained a pressure between 5 and 8 x 10^{-4}torr during irradiation. Some of the cells were illuminated during irradiation while others were dark. At NRL the solar cell temperatures ranged from 21 to 29°C in one chamber and from 41° to 48°C in the other. No temperature control was attempted throughout the experiment. Daily readings were made of the vacuum, temperature, and illumination voltage.

The experiment sample matrix is shown in Table I. It is seen that most data points refer to only one sample. This is one of the main deficiencies of this particular experiment, as far as assigning statistical significance to the data. Because of cell breakage and removal of cells for study over the time of the experiment, new cells were added at various intervals. This matrix does not reflect the fact that the cells are at 6 different values of fluence and were manufactured at various periods. Another difficulty to accurate interpretation of data is the lack of any control cells in the experiment. It is impossible of course to place completely shielded cells in the radiation chambers. The cylindrical dimensions of 3 in. diameter and 9 in. high preclude this. It would have been useful to expose cells to the same non-radiation environment (i.e. vacuum and temperature) as the irradiated cells and to include them in the periodic measurements.

Such cells might indicate a change in characteristics as a function of temperature, or serve to define the accuracy of measurements on all cells. Material to be used in the radiation chamber (e.g. wire insulation) must be carefully chosen to prevent undesirable reaction to the gamma rays.

At the time of transference to NRL the cells had received a total accumulated dose up to a maximum of 3.74×10^{15} 1 MeV e/cm^2 equivalent. The additional 5 months irradiation at NRL added a dose of 5.5×10^{14} 1 MeV e/cm^2 equivalent. Measurements of the I-V curves were made monthly under a tungsten light source of 100 mW/cm^2 solar equivalent with a 3 cm water filter.

We observed some scattering in the data points which was generally much less than previously reported. Also our tungsten light gave I_{sc} values about 12% less than the EMR measurements.

We agree with Fang[3] that it is not possible to establish specific values of significant differences between cell types from the data of this experiment. He did report several general observations with respect to the EMR work. A few general conclusions can be made with respect to the NRL portion of the experiment.

(1) The float-zone lithium-diffused cells are almost stabilized with respect to further radiation damage after a dose of 4×10^{15} e/cm^2, whereas the Lopex and crucible-grown lithium cells are still degrading slightly.

TABLE I EXPERIMENT SAMPLE MATRIX

Cell Type	Other Data	MFR	Number Irradiated				
			25°C Light	25°C Dark	43°C Light	43°C Dark	
Lithium P/N Float Zone		TI		3	2	1	
		HEL	3	1			
Lithium P/N Lopex		TI	2+1*	3+1*		2	
		CEN		3		1	
Lithium P/N Crucible Grown		TI	2	3+1*	2	1	
		HEL	2				
	As Doped	CEN	3	1			
	Sb Doped	CEN	2	1			
N/P Production		HEL	2	1			
		CEN	1	1			
	1 Mil Int. Coverslip	CEN	1	1			

*Cells from same manufacturer but different runs.

Final fluences range from 2.1 to 4.3 x 10^{15} e/cm^2.

(2) The n/p commercial cells continue to degrade at a rate about equal to the worst of the lithium-diffused cells.

(3) Tungsten efficiencies for lithium cells at the dose of 4×10^{15} e/cm^2 range from 4.6 to 7.7%.

(4) Probably the most important fact is that there is a continuing damage rate in some kinds of lithium-diffused solar cells which extends over a long period of time, (as also noted by Fang).

2.3 SOLAR CELL CONTACTS

There is a continual effort in solar cell research to improve the overall efficiency of the type of solar cells being used in space probes. One of the major goals is the construction of low resistance, time-stable, metal-semiconductor contacts to pass electrical power from the cell. The contacts ideally should be light, mechanically and electrically reliable, and reasonably economic. The use of solar cells on deep space probes puts an additional requirement on the problem of reliable contacts, namely that of performing well over wide temperature ranges. For example, contacts that are ohmic at room temperature may not be ohmic at the 125°K estimated as the working temperature of the Jupiter probe. Wide temperature excursions may also cause contact failure because of the different coefficients of thermal expansion of the silicon and contact material. Presently the most commonly used contacts are formed by evaporation. This program will investigate the development of improved silicon solar cell contacts through the use of ion implantation techniques.

A 35 KeV bench accelerator was designed and constructed to produce ion beams from atomic species that exist in gaseous form. The n- and p-type dopants of special interest are phosphorus and boron, which are obtained from phosphine (PH_3) and boron trichloride (BCl_3), respectively. It may eventually be shown that other gases such as oxygen and nitrogen may have advantageous effects as dopants; the introduction of nitrogen as a dopant can only be accomplished by implantation (it exists as a diatomic molecule with a high bonding strength (8.9 eV) and hence is too big to enter silicon by diffusion). The noble gases are conveniently and easily handled and are used for calibration purposes in implantation studies.

A schematic of the ion accelerator is shown in Figure 9. Gas is bled continuously into the quartz bottle at a pressure of $\sim 2 \times 10^{-2}$ torr, and is ionized by a strong R.F. field. The ionization probability is increased by the application of an axial magnetic field. Positive ions are extracted from the induced plasma and accelerated through a series of electrostatic focusing lenses. The accelerating systems can be adjusted to give an energing ion beam energy from 5 to 35 KeV.

The ion beam thus formed is well defined and slightly divergent. It is projected into the center of the gap of a 6 inch circular analyzing magnet and parallel to the pole faces. This particular geometrical alignment of the beam with the magnet is a requirement for proper focusing. The alignment is effected by means of suitable slits and an electrostatic lens placed

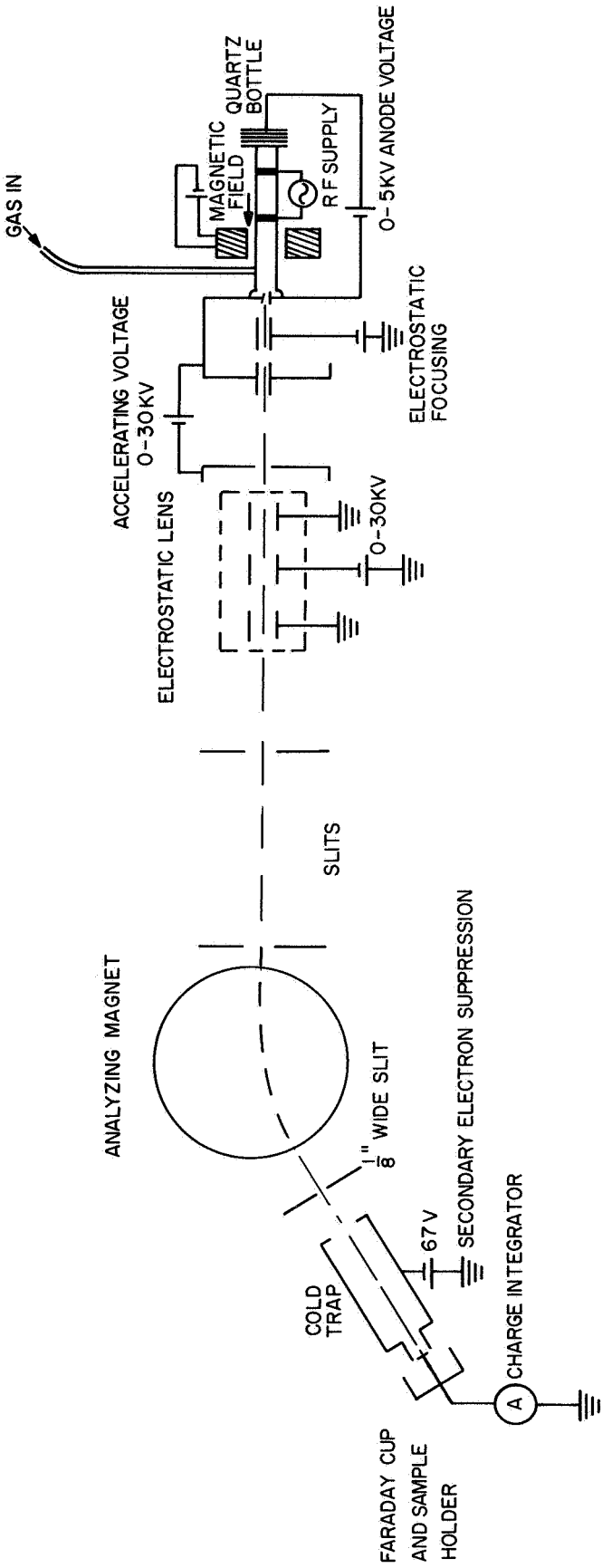

Figure 9. Schematic diagram of the 35 KeV ion accelerator.

near the ion source. With the present arrangement ions up to mass 25 AMU can be handled; this range can be extended by the use of smaller pole gap.

The magnetic field is adjusted so that the ions of interest pass through a 1/8" slit before striking the target. The target serves as a charge collector. Beams of 2 cm^2 in area are obtained using the above procedure. An in-line LN_2 cold trap, which prevents sample contamination from back diffusion of pump oils, is also negatively biased to suppress secondary electrons. The ion optics are such that a resolution (defined as $\frac{m}{\Delta m}$) of 25 can be obtained for ion currents in the nanoampere range. A mass scan using BCl_3 is shown in Figure 10. The corrosive nature of BCl_3 produced some minor problems in the gas handling system. The gas inlet leak valve corroded and was therefore replaced with a system capable of handling corrosive materials.

The recent implantation work has been focused on boron, or p-type dopant, which will be used to improve the contact on the back side (p-side) of a standard n-on-p solar cell. The gas BCl_3 has been used to obtain boron beams up to 40 nA on a 2 cm^2 target. This current is sufficiently high to degenerately dope silicon in a matter of minutes. To determine the doping effect of ion implanted boron the resistivity of the surface of a Schottky barrier diode was investigated. Past bombardment annealing of the samples to a few hundred degrees Centigrade produced predictable changes in the resistivity. The resistivity changed in the p-direction by an amount that would be expected from the given dose of the implanted boron ions.

At the present time, the technique is restricted to dopants that exist in gaseous form. A survey has been conducted on the sources available to handle most elements of interest. The sputtering type source is very effective with metals which have a high sputtering yield. Materials with low melting temperatures can be handled by evaporation, while high melting temperature materials can be obtained in gaseous form by the use of a reactive gas ($C Cl_4$). Each type of source has its specific advantage with respect to producing ions and limitations with respect to power requirements. The power requirements of the sputtering source are such that it can be used in the NRL 5 MeV Van de Graaff, whereas the evaporation and reactive gas type can not. The sputtering source, however, is limited in the type of materials that can be handled. We are considering the purchase of a commercial source and are also developing a sputtering-type source.

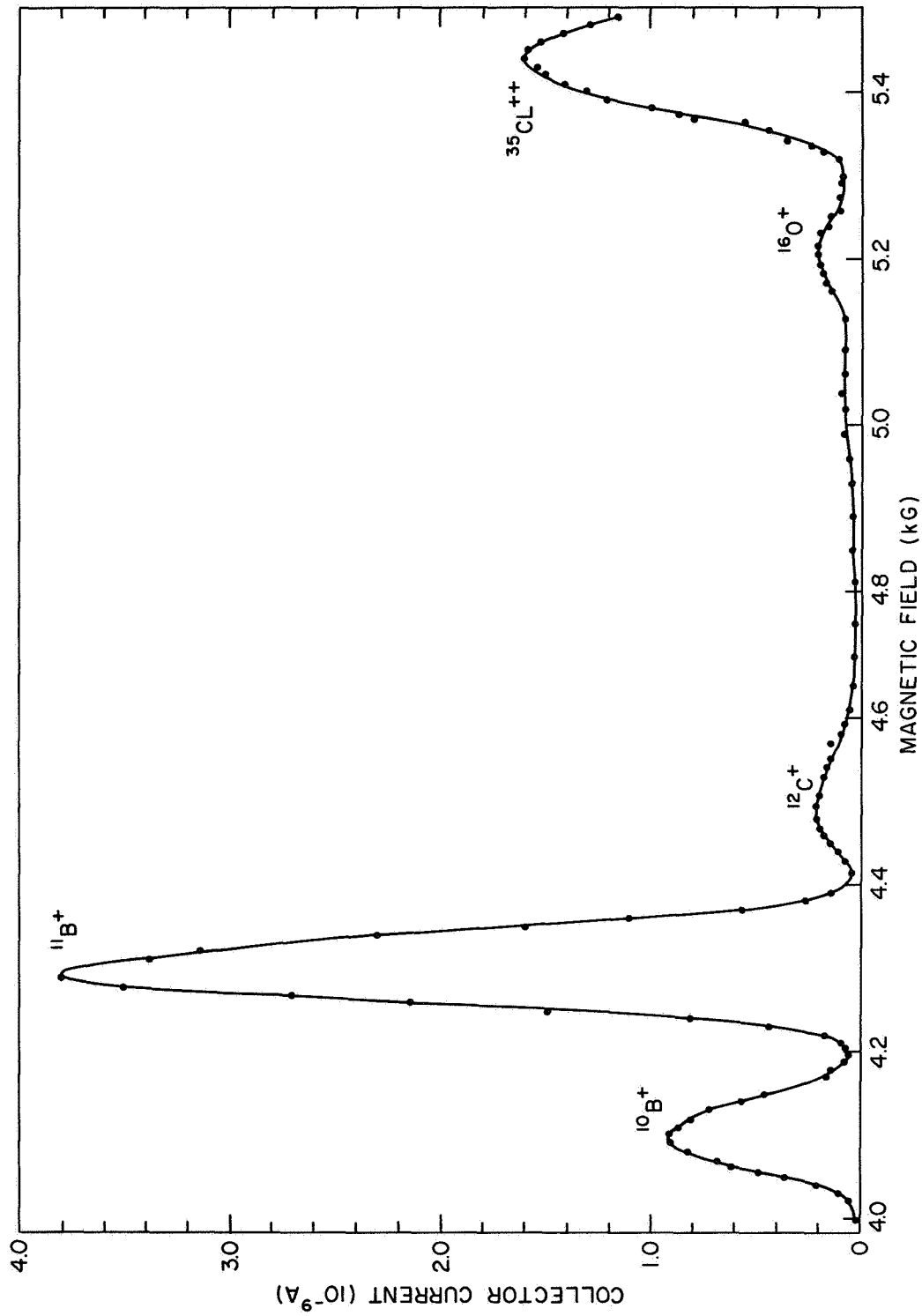

Figure 10. Mass scan obtained from the 35 KeV accelerator using BCL_3. The ion energy is 20 KeV.

2.4 ELECTRICAL CHARACTERISTICS OF SILICON SOLAR CELLS AT LOW TEMPERATURE

NRL was requested to study the properties of solar cells at low temperatures and intensities in coordination with programs at NASA-AMES and NASA-GSFC. There is an urgent need for such information for Jupiter probes and other outer planetary experiments. Jupiter is 5.20 AU from the sun, with a resulting solar intensity of only 5.2 mW/cm^2. The temperature of a solar cell array in the Jovian environment is predicted to be about 125°K. A pre-

A preliminary study[4] using nine silicon solar cells of three different types was carried out at light intensities ranging from 1 to 140 mW/cm^2 over a temperature range of 85° to 300°K. The cells comprised three each of 1 Ω- cm p/n, 1 Ω- cm n/p, and 10 Ω- cm n/p. The group of 10 Ω- cm cells contained samples from two vendors. The single cell from one manufacturer had very different I-V characteristics from the other cells at low temperatures.

Three solar cells were mounted on the cold finger of a liquid helium dewar as shown in Figure 11. Measurements were made in sequence on cells by turning the dewar to illuminate the cells through supersil windows. A sapphire slab was sandwiched between the solar cell and the brass cold finger to prevent cell breakage because of unmatched thermal expansion coefficients. One side of the sapphire was metallized and soldered to the heat sink. The cell was then cemented to the sapphire with GE 7031 varnish. The cell was allowed to overhang the sapphire by one millimeter to allow for soldering the electrical connection and a copper-constant on thermocouple to the back of the cell.

The solar cell I-V curves were measured under illumination from a Spectrosun X-25 solar simulator. Neutral density filters were interposed in the light path to obtain the low intensity levels.

From the results of this study, the cells can be grouped into two categories. The first of these includes the three 1 Ω-cm p/n cells and one of the 10 Ω-cm n/p cells. These cells exhibit a non-ohmic behavior at temperatures below about 200°K. The remainder of the cells have good diode characteristics at the lowest temperatures reached. All cells show gradual increases in efficiency as the temperature is lowered. The amount of efficiency increase is a function of illumination. The largest increase occurs at 140 mW/cm^2 with practically no change at 1 mW/cm^2.

This program is being continued in cooperation with NASA-AMES and NASA-GSFC. Ames has provided six 2 x 2 cm silicon solar cells mounted on kovar substrates. These cells will be measured under conditions similar to those above.

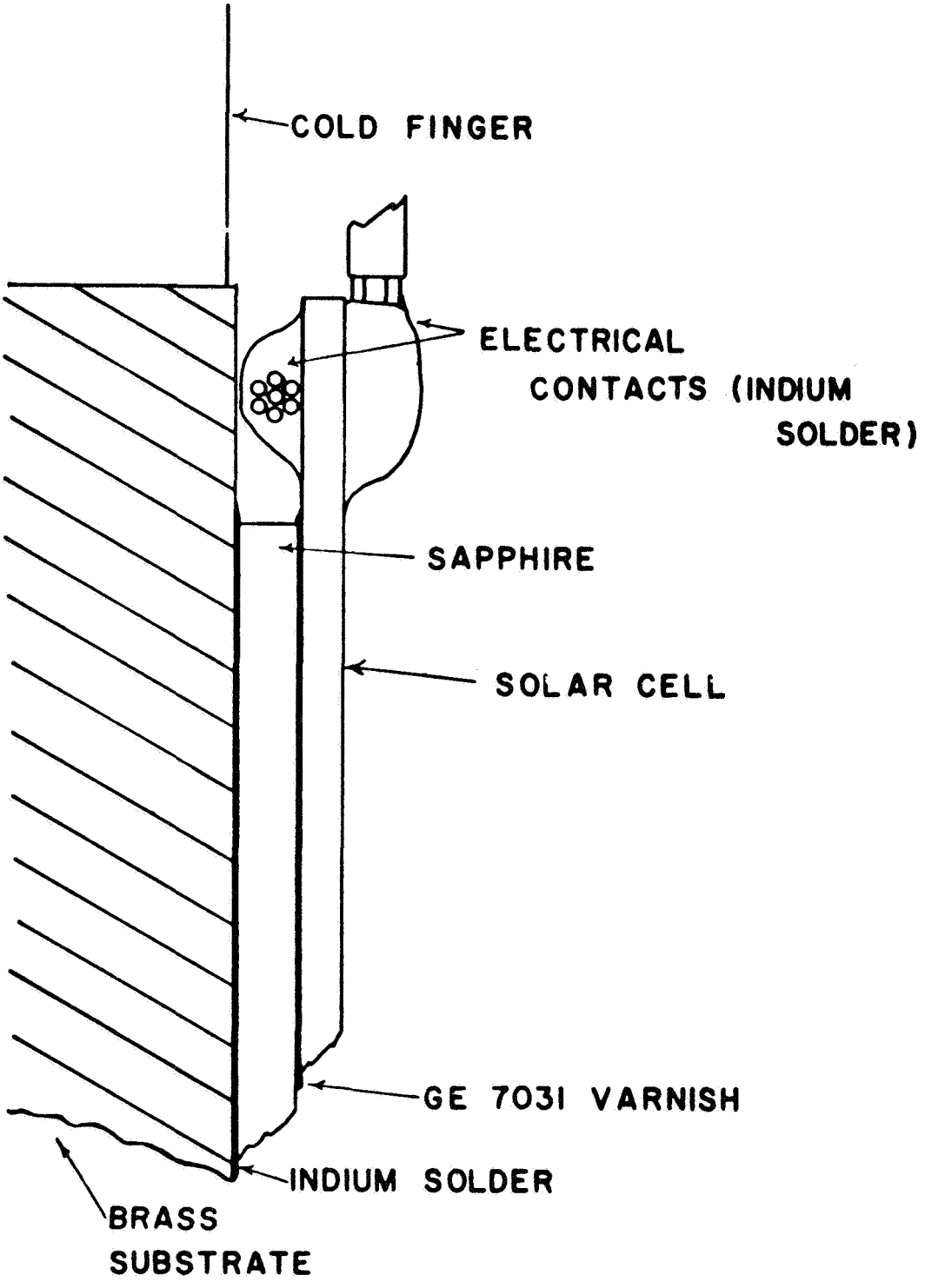

Figure 11. Schematic diagram of the solar cell mounting for low temperature measurements.

2.5 ANALYSIS OF SOLAR CELL I-V CHARACTERISTICS

As an approach to analyzing solar cell I-V curves, a computer program has been written to fit experimental I-V data to the solar cell equation. The computer program has been adapted from a general least-squares program[5] which performs a least squares analysis for both nonlinear and linear functions. The maximum neighborhood method of Marquardt[6] is used. This method provides an optimum interpolation between the Taylor series method and the steepest-descent or gradient method. Convergence is assured at every interaction and speed of computation is maximized.

In addition, the program provides a statistical analysis of the fit. The statistical information provided is:

(1) the unbiased standard deviation of the function,

(2) the multiple correlation matrix of the parameters,

(3) the standard deviation of the parameters,

(4) the contour standard deviation,

(5) ellipsoidal estimates of the parameters,

(6) confidence limits on the value of the function.

Plotting subroutines are also provided which graph the experimental data, the best fit to this data, the 95% confidence limits on the data, and an error curve.

The solar cell equation is usually written in the form

$$I = I_L - I_o \left[\exp\left(\frac{V - IR_s}{V_o} \right) - 1 \right] \qquad (1)$$

where $V_o = AkT$

and A = a constant with value between 1 & 3

k = Boltzmann's constant (8.616×10^{-5} eV/^oK)

T = temperature (^oK)

I = load current

V = voltage across the cell

I_L = light generated current

I_o = reverse diode saturation current

R_s = effective series resistance of the cell

Equation (1) can be rewritten as

$$V = V_o \ell n\left(1 + \frac{I_L - I}{I_o}\right) - IR_s . \tag{2}$$

The computer program as described above can be utilized to obtain a best fit of I-V data to Eq. (2), by treating I_L, I_o, V_o, and R_s as adjustable parameters. Since the short-circuit current, I_{sc}, and open-circuit voltage, V_{oc} are accurately measured, the number of adjustable parameters can be reduced from 4 to 2. The choice of the two parameters to be varied is arbitrary. For example, if I_L and I_o are chosen to be variable, Eq. (2) can be written as:

$$V = \frac{V_{oc}}{\ell n\left(1 + \frac{I_L}{I_o}\right)} \ell n\left(1 + \frac{I_L - I}{I_o}\right) - \frac{I}{I_{sc}} \ell n \left(1 + \frac{I_L - I_{sc}}{I_o}\right). \tag{3}$$

The parameters A and R can be calculated from the values of I_o and I_L which give a best fit of the data to Eq. (3); that is,

$$A = \frac{V_{oc}}{kT \ \ell n \left(1 + \frac{I_L}{I_o}\right)} \tag{4}$$

and

$$R = \frac{AkT}{I_{sc}} \ell n \left(1 + \frac{I_L - I_{sc}}{I_o}\right) \tag{5}$$

Alternatively, R_s and V_o can be chosen to be variable and Eq. (2) becomes:

$$V = V_o \ell n \left\{ 1 + \left[\exp\left(\frac{V_{oc} + I_{sc} R_s}{V_o} \right) - 1 \right] \left[1 - I/I_{sc} \right] \right\} - \left(I_{sc} - I R_s \right). \quad (6)$$

The parameters A, I_o, and I_L can then be calculated from the best fit values of V_o and R_s:

$$A = V_o/kT , \quad (7)$$

$$I_o = I_{sc} / \left[\exp\left(V_{oc}/V_o \right) - \exp\left(-I_{sc} R_s/V_o \right) \right] \quad (8)$$

and

$$I_L = I_{sc} + I_o \left[\exp\left(-I_{sc} R_s/V_o \right) + 1 \right] . \quad (9)$$

The parametric study of the solar cell I-V curves has two applications. First, the statistical analysis gives an indication as to the applicability of this simple solar cell equation. Second, additional environmental factors such as temperature and irradiation fluence can be studied.

An example of the type of fit which can be obtained with the nonlinear least squares program is given in Figure 12. The overall fit can be seen to be quite good.

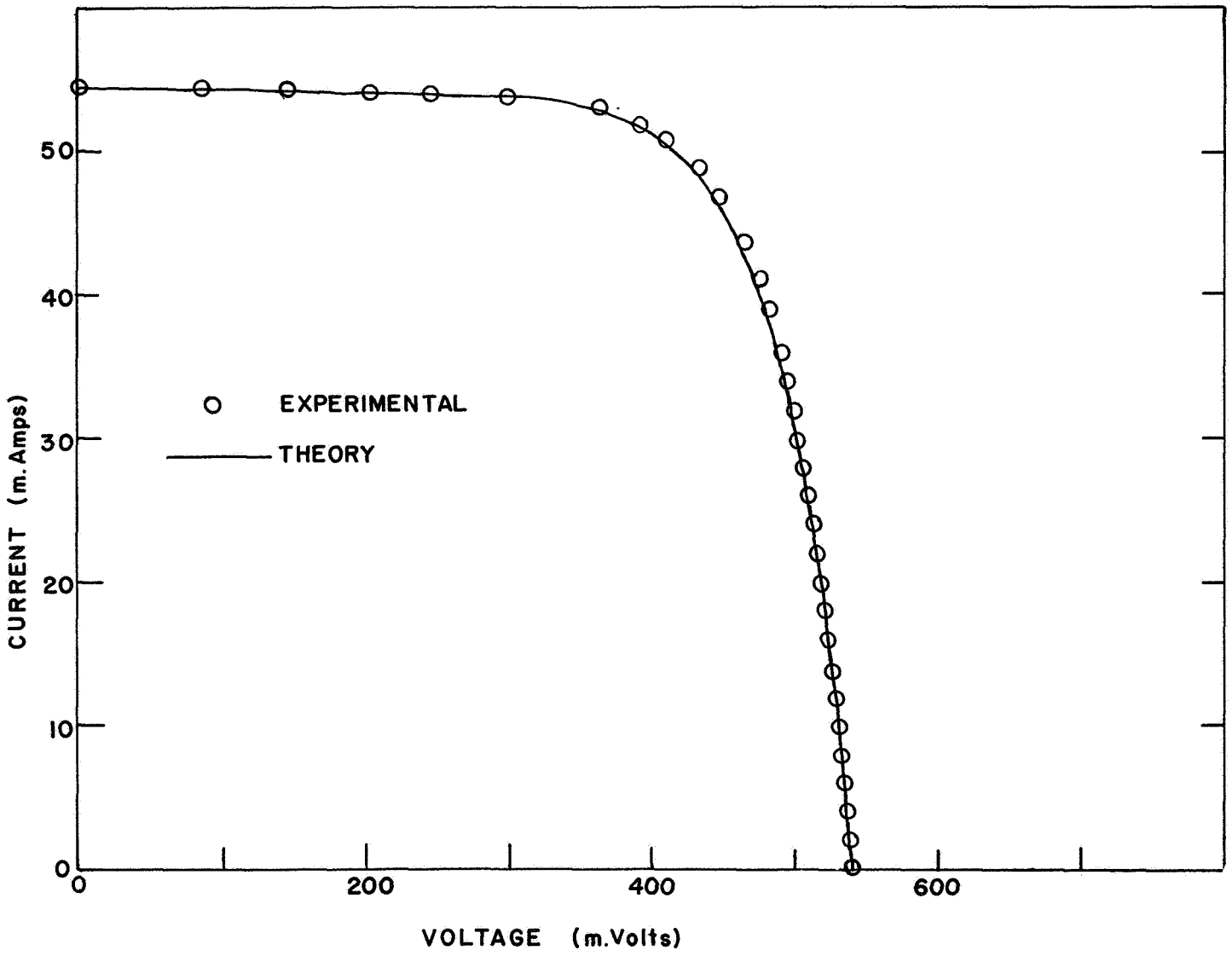

Figure 12. An example of the least-squares fit to the solar cell I-V characteristics using the lumped constant model (Eq. 6). The fit is excellent except for the region of the "knee" of the curve.

2.6 REVIEW OF "HANDBOOK OF SPACE ENVIRONMENTAL EFFECTS ON SOLAR CELL POWER SYSTEMS"

The Handbook of Space Environmental Effects on Solar Cell Power Systems released in January 1968 represents a revision, up-dating and expansion of an earlier handbook published in July 1963 as NASA Report SP-3007. The revised Handbook treats in more detail then its predecessor subjects such as the Theory of the Solar Cell, Radiation Damage to Solar Cells, the Space Radiation Environment, Satellite Test Data and Design Methods for Solar Cell Power Systems, Radiation Effects in Coverslides and Adhesives, and Radiation Effects on Power Conversion and Regulation Equipment. The last two topics were included as appendices in the earlier Handbook. New chapter headings include Instrumentation Techniques for Measuring Solar Cell Panels, Radiation Shielding of Solar Cells, and the Effect of Meteoroids on Solar Cell Arrays.

The present review will be restricted to the Theory of the Solar Cell (Chapter II) , and Instrumentation Techniques for Measuring Solar Cell Parameters (Chapter III). The review of Chapter IV, Radiation Damage to Solar Cells, will be deferred to a later report.

The Theory of the Silicon Solar Cell as outlined in the revised Handbook represents a vast improvement over the discussion presented in the earlier version of the Handbook. This section generally provides sufficient tutorial background relating to the photovoltaic effect for the engineer whose principal interest is the design of solar cell power systems for space applications. However, references to more detailed treatments of the physics of the p-n junction and the photovoltaic effect should be provided, e.g. the excellent discussion by S. S. L. Chang in "Energy Conversion", Prentice Hall 1963, Chapt. 6.

The introduction of the solar cell equation, Eq. II-2, provides an excellent opportunity to present a brief description of the more important solar cell parameters, e.g. the I-V characteristics, the short-circuit current, the open-circuit voltage, the maximum power output, and the spectral response. At this time, some of the interrelationships between the various parameters should also be treated, e.g., the relation between the minority carrier diffusion length and short-circuit current referred to on page II-7. It would also be helpful to include some of the quantitative results mentioned in Refs. 161, 218 and 22, particularly since the latter two references are unpublished contract reports rather than journal articles generally available in the open literature.

An early introduction of the solar cell parameters would also afford an opportunity to examine the dependence of these parameters on the intensity and spectral distribution of light and on the temperature. Such dependence is suggested in the Handbook on Page II-7 by statements such as, "the parameters I_o, A, and R_s are found to depend on temperature" and "the light-generated current I_L is a function of the intensity and spectral distribution of the light source". But these statements are unsupported by quantitative description. Some experimental data are cited in connection with the dependence of the I-V characteristics and power output of unirradiated cells in Chapter IV. In addition, the dependence of I_o, I_L, V_{oc}, A, R_s, and the I-V characteristics on the light intensity are alluded to on page III-9 in connection with measurement techniques. This incomplete treatment of this subject weakens the worth of the Handbook at a time when planned space missions to other planets require this very necessary information. A space power designer charged with a mission to Jupiter or Venus will be extremely interested in the dependence of solar cells properties on temperature and light intensity and should find some guidance from the Handbook. In the absence of experimental data, some theoretical expectations should be included. Furthermore, the available information should be presented in one part of the Handbook.

The purpose of Chapter III is to summarize instrumentation techniques for the measurement of the various solar cell parameters and to present an account of calibration methods for using different light sources (natural and artificial). As pointed out earlier, this Section appears for the first time in the revised Handbook. The present treatment is generally quite useful and complete in details for the experimenter as well as the designer who may be forced by operational urgency to carry out measurements. However, the continuity of the Chapter is somewhat marred by the necessity of introducing and defining the various solar cell parameters prior to a description of the appropriate measurement techniques. A previous definition of these parameters in Chapter II (or another separate Chapter) would eliminate the need for descriptive material which is not directly related to instrumentation.

A more serious deficiency is the lack of data for unirradiated cells as a function of light source. Although there is an exhaustive treatment of the variety of sources in standard use, e.g., tungsten bulbs, carbon arcs, xenon arcs, solar simulators, sunlight (at Table Mountain, balloon and airplane flights), nowhere is there any comparison of cell parameters for a single group of cells carefully measured under all of the various light sources. Much of the solar cell data found in the literature is difficult to evaluate or to correlate because of differences in light sources. The Handbook should be expected to reduce some of the confusion which may arise from the use of different light sources.

Another omission from Chapter III is a treatment of the important subject of measurement accuracy. It is well known that a selected lot of solar cells whose fabrication has been carefully controlled by the manufacturer and whose initial properties are well matched may upon irradiation exhibit widely varying behavior. It is necessary that a sufficiently large number of samples be chosen for a given experiment in order that the results be statistically significant. A discussion of this topic with directions for planning a sample matrix for a typical radiation experiment might be in order.

It is also noted that no techniques are described for measuring the properties of solar cells as a function as temperature. The kind of measurement has assumed an increased importance in the light of outer planetary explorations. The various types of variable temperature cell holders and dewars which have been utilized for such studies might be reviewed, as well as the manner of mounting the solar cells to the heat sink.

3.0 CONCLUSIONS

From the study of charge carrier annealing at 300°K in lithium-diffused electron irradiated silicon a decrease in the free lithium and lithium-oxygen pair concentrations was observed concurrently with a decrease in acceptor concentration. The loss in total donor concentration was approximately twice the loss in acceptor concentration. The radiation-induced acceptor defects became electrically neutral upon annealing at 300°K. A deep donor level whose concentration was unaffected by annealing was observed at 0.15 eV below the conduction band.

The low flux gamma irradiation of lithium diffused solar cells has disclosed the existence of a continuous damage process in some types of lithium-silicon solar cells over long periods of irradiation. This appears more predominantly in crucible grown and Lopex silicon than in float-zone silicon. The present experiment encompassed too many variable parameters with insufficient numbers of samples to permit more specific evaluation. Carefully planned experiments will be required to establish quantitative data.

The work on ion implantation for improving solar cell contacts has demonstrated the successful production of a focused, controlled boron beam from an ion accelerator. This boron beam (which is capable of varying in energy from 5 to 35 KeV) was used to implant boron in a Schottky barrier diode, thereby changing the resistivity in such manner as to verify the implantation of boron ions. A metal ion source for solar cell contact formation is being developed.

The measurement of solar cell efficiency over the range of room temperature down to liquid nitrogen temperature has revealed that in some types of silicon solar cells, the efficiency improves up to 16% at the low temperature end. Results also show that solar cell contacts may become a problem in some silicon cells (e.g. 1 ohm-cm p/n and a 10 ohm-cm n/p) at low temperatures. The small amount of data so far obtained are considered to indicate qualitative results only.

A general least-squares program has been adapted to provide an analysis of solar cell I-V curves. It appears that this method of analysis will be useful in a parametric study of solar cell parameters as a function of temperature and radiation fluence.

A review of Chapters II and III in the "Handbook of Space Environmental Effects in Solar Cell Power Systems" was made. In general, these portions of the Handbook are a great improvement over those in the first edition in clarity and inclusiveness.

It is suggested that the introduction of certain solar cell parameter definitions together with their functional dependencies would be valuable near the beginning of the Handbook. This is a need also for a more detailed treatment of temperature effects on solar cell properties and a description of the experimental techniques necessary for temperature effect measurements. It would be valuable to discuss the design of a "typical" radiation experiment, with the planning of the sample matrix and discussion of experimental accuracy and statistics.

4.0 RECOMMENDATIONS

The Hall coefficient measurements have proven to be extremely useful in analyzing the interaction of lithium with radiation defects in silicon. This study will continue with particular attention given to identifying the deep donor level at E_c-0.15 eV, studying the formation of a lithium-vacancy complex, and investigating the dependence of annealing phenomena on donor concentrations.

The low flux Co^{60} gamma experiment is being completely redesigned, using new cells with fewer experimental parameters. The proposed experiment sample matrix is shown in Table II. The level of radiation will be equivalent to a flux of 3×10^{12} e/cm^2 per day. This experiment will continue for an indefinite time, in as long as useful data is obtained.

The solar cell contact investigations will study the formation of metallic contacts by evaporating, sputtering, and ion implantation techniques. A lot of 75 Centralab n/p solar cells (without anti-reflective coatings) have been received for this program. Some of these cells have factory-applied Ag-Ti contacts, others are without contacts.

Solar cell measurements at low temperatures and low intensities from a solar simulator will be made in cooperation with programs at NASA-Ames and NASA-Goddard. Analysis of data will be performed by the computer curve-fitting technique discussed in Section 2.5 of this report. The spectral response of solar cells will be studied also as a function of temperature and intensity. Finally, electron irradiation of a variety of cells with complete temperature and intensity measurements will be performed to provide a quantitative evaluation for power system design and prediction.

The critique of the Handbook of Space Environmental Effects on Solar Cell Power Systems will continue. The next portion to be reviewed will be Chapter IV, Radiation Damage to Solar Cells, which is the longest and perhaps most important section of the book.

TABLE II PROPOSED EXPERIMENT SAMPLE MATRIX

Cell Type	Other Data	Number Irradiated		Controls
		35°C Light	60°C Light	60°C Light
Lithium P/N Float Zone	Low Li Concentration	5	5	3
	High Li Concentration	5	5	3
Lithium P/N Crucible	Low Li Concentration	5	5	3
	High Li Concentration	5	5	3
N/P Production	Centralab	5	5	5

All lithium cells are fabricated by Heliotek.

All cells will be gamma-irradiated in tungsten light and have a 10 ohm load resistor with a load voltage of 0.30 to 0.35 volt. The control cells will also be resistive loaded.

5.0 NEW TECHNOLOGY

1. Technique for mounting a silicon solar cell to dewar cold finger for photovoltaic measurements at temperatures from 300°K to 80°K.

   Originated by R. J. Lambert.

   Described in Semiannual Report for Solar Cell Research, p. 24, 15 April 1969.

6.0 PUBLICATIONS (Written and Oral)

1. "Characteristics of Solar Cells at Cryogenic Temperatures", R. J. Lambert, IEEE Photovoltaic Specialists Conference, 19-21 November 1968, Pasadena, California.

2. "Low Energy Proton Damage in Silicon Solar Cells", R. L. Statler and D. J. Curtin (Comsat), IEEE Photovoltaic Specialists Conference, 19-21 November 1968, Pasadena, California.

3. "Oxygen Sticking Coefficients on Clean (111) Silicon Surfaces", C. A. Carosella and J. Comas, Bull. Am. Phys. Soc., 13, 1455 (1968).

4. Semiannual Report to Solar Working Group, IAPG, 18 November 1968.

5. "Radiation Effects in Silicon Solar Cells", R. L. Statler, International Conference on Physics and Technology of Nonmetallic Crystals, New Delhi, India, 13-17 January 1969.

6. "Analysis of Radiation Damage in Silicon by Thermal Annealing of Solar Cells", B. J. Faraday, International Conference on the Physics and Technology of Nonmetallic Crystals, New Delhi, India, 13-17 January 1969.

7. "Electron Irradiation of Lithium-Doped Silicon at Low Temperatures", J. E. Stannard, Bull. Am. Phys. Soc., 14 326 (1969).

8. "Analysis of Radiation Damage in Silicon by Thermal Annealing of Solar Cells", B. J. Faraday, NRL Report of Progress, February 1969.

9. "300°K Annealing of Electron Damage in Lithium-Doped Silicon", J. E. Stannard, presented at Review of Progress in Lithium-Diffusion Solar Cells, JPL, Pasadena, Calif., 8 April 1969.

10. "Status of Semiconductor and Solar Cell Research at NRL", R. L. Statler, presented at Solar Working Group, IAPG, Washington, D. C., 18 March 1969.

7.0 REFERENCES

1. J. D. Carter, Jr. and R. G. Downing, Semiannual Prog. Rept., Contract NAS 5-10322, TRW Systems, 28 August 1966.

2. R. A. Schmidt, "Degradation of Solar Cells", Final Report, Task 713-2220, Electro-Mechanical Research, Inc., 31 August 1968.

3. P. H. Fang, "Gamma Irradiation of Lithium Silicon Solar Cells", Conf. Record of the Seventh Photovoltaic Specialists Conference, p. 113, 19-21 November 1968.

4. R. J. Lambert, "Characteristics of Solar Cells at Low Temperatures", Conf. Record of the Seventh Photovoltaic Specialists Conference, p. 97, 19-21 November 1968.

5. W. E. Daniels, Jr., "General Least Squares with Statistics", Technical Report No. 579, University of Maryland, Dept. of Physics and Astronomy, July 1966.

6. D. W. Marquardt, J. Soc. Indust. Appl. Math. 11 431 (1963).